

Reversible protective and consolidating coatings for the ancient iron joints at the Acropolis monuments

Giasemi Frantzi¹, Michail Delagrammatikas², Olga Papadopoulou², Charalampos Titakis², Eleni Aggelakopoulou¹, Panayota Vassiliou²

¹ Acropolis Restoration Service (YSMA), 10 Polygnotou Str., 105 55 Athens, Greece

² Laboratory of Physical Chemistry, Department of Materials Science / School of Chemical Engineering, National Technical University of Athens (NTUA), 9 Iroon Polytechniou Str., 15780 Athens, Greece

ABSTRACT

This work presents a corpus of measurement methodologies utilized during a multidisciplinary project, aiming at the protection and conservation of ancient steel joints (clamps and dowels) of the Acropolis monuments, undertaken by the Acropolis Restoration Service (YSMA). The Laboratory of Physical Chemistry of the National Technical University of Athens collaborated with YSMA in designing and evaluating laboratory scale and field experiments, aiming in testing conservation materials.

The first phase involved the application of seven coating systems on uncorroded metal coupons. The application characteristics, physicochemical properties (colour, gloss, hydrophobicity), and the protection performance against accelerated corrosion and polymer photo-oxidation were measured. Poligen CE12 and Paraloid B67 +2 % nano-alumina were selected as the two most suitable materials for pilot applications on corroded steel joints and outdoor field exposure at the monument site.

The assessment of the two coatings reversibility and of the corroded surfaces chemical alteration was undertaken by Raman spectroscopy analyses and orthophotographic documentation. During the 1-year field exposure, the corrosion development was retarded, but some local events of active corrosion could not be prevented. The joint areas coated with Paraloid B67 enhanced with 2% nano-alumina enabled more uniform application on corroded surfaces and exhibited better corrosion protection. In case of Poligen CE12, the nature of corrosion products indicated local acceleration of corrosion reactions.

Section: RESEARCH PAPER

Keywords: Paraloid; Poligen; atmospheric corrosion; polymer coatings; ancient iron; Raman spectroscopy

Citation: Giasemi Frantzi, Michail Delagrammatikas, Olga Papadopoulou, Charalampos Titakis, Eleni Aggelakopoulou, Panayota Vassiliou, Reversible protective and consolidating coatings for the ancient iron joints at the Acropolis monuments, Acta IMEKO, vol. 11, no. 4, article 14, December 2022, identifier: IMEKO-ACTA-11 (2022)-04-14

Section Editor: Leonardo Iannucci, Politecnico di Torino, Italy

Received July 11, 2022; **In final form** December 15, 2022; **Published** December 2022

Copyright: This is an open-access article distributed under the terms of the Creative Commons Attribution 3.0 License, which permits unrestricted use, distribution, and reproduction in any medium, provided the original author and source are credited.

Corresponding author: Michail Delagrammatikas, e-mail: mdel@mail.ntua.gr

1. INTRODUCTION

Numerous multi-analytical case studies on atmospheric corrosion of ancient and historic iron and steel, published during the last decades, have offered the general knowledge and understanding on complex stratification and morphological patterns resulting from long-term burial in soil [1], [2] or from atmospheric exposure [3]-[6]. The study of atmospheric corrosion mechanisms in particular - wet and dry cycles inside Fe corrosion layers, as well as the chemical composition of sub-layers- allowed the modeling of long-term atmospheric corrosion of iron, as Hærlé et al. [7] have attempted for indoor environments.

The preservation of cultural heritage metals (artefacts, monument elements, and industrial heritage elements) involves multiple specialized preventive conservation protocols, interventive surface treatments (washing, mechanical, chemical or electrolytic cleaning, stabilization), consolidation and conservation procedures by means of coatings, adhesives and corrosion inhibitors. The framework of all well-established practices and of any new developments of this interdisciplinary scientific area is based on specific criteria and considerations that should not put at risk or compromise the aesthetic, chemical, and mechanical integrity of metals [8].

The aim of this paper is twofold: (i) to report the systematic methodology of the restoration and maintenance project, targeted on consolidation and corrosion protection of

monument joints and the multi-step evaluation of products and systems before the final application on monument elements and (ii) to contribute to the broader study of application and protection properties of conservation coatings, when applied on heavily corroded steel surfaces exposed in natural outdoor atmospheric environments.

The paper is organised in five sections. Section 1 comprises the afore introduction. Section 2 briefly presents the State-of-the-Art, with reference to bibliographic sources. Section 3 describes the material and the methods that were used in this research, while Section 4 comprises of presentation of results and discussion. Following Section 5, presents in a comprehensive way the conclusions and future planned work.

2. STATE OF THE ART

There is a growing interest in the formulation of new conservation coatings for cultural heritage materials with advanced features: reversible, with extended operational life, UV resistant and water repellent, eco-friendly, non-toxic for the user [9]. The latest developments in this field, with some promising results, concern wet waxes (aqueous emulsions), silane coatings, triazole derivatives, fluoro-polymers and some nano-composites [9], [10]. None of these products has been proposed for general application on heritage artworks and monument elements so far. The traditional polymer conservation materials - i.e. acrylic resins and waxes- are still in use and considered reliable given their well known limitations [11]. The challenge to assess the degradation mechanisms and overall performance of novel and traditional coatings in various environmental conditions and substrates over time is an open research field for conservators and corrosionists.

According to a survey research conducted by Argyropoulos et al. [12] dating back to 2007, Paraloid coatings and waxes are very popular for conservation of museum ferrous metal collections, both in Greece and in all European countries [12], [13]. In Mediterranean countries in general it is common for conservators and restorers to use wax over acrylic coatings for the protection of ironwork.

Very limited experimental data is available on the application of acrylic coatings and waxes on heavily corroded surfaces, which are not museum exhibits in a controlled environment but directly exposed on site outdoors to all weather conditions, and this is also the case for the physicochemical degradation mechanisms of conservation polymer materials in general. Most of the times, the long-term behaviour of conservation polymers is assessed from the empirical knowledge of experienced conservators - from relevant restoration and conservation works- or from published laboratory reports from artificial ageing tests of coated metal coupons [12], [14], [15].

Swartz et al. [16] have tested the performance of two commercial conservation waxes (Renaissance Wax and Butcher's Boston Polish Amber Paste wax) on bronze and steel specimens at various time intervals, both by laboratory UV-ageing tests as well as exposure in outdoor environment. Wax coatings on steel exhibit a very short lifetime and are particularly prone to polymer chain oxidation cross-linking (with the additional consequence of less easy removal of the aged wax coating).

The wax layers were found to fail in a period of less than 6 months of outdoor exposure and within 250-750 h of UV-B radiation. The atmospheric field exposure leads to faster and non-uniform surface deterioration and some of the produced oxidation products in aged waxes are believed to enhance corrosion rates due to their lower hydrophobicity.

Cano et al. [17] evaluated by electrochemical methods the protective properties of Poligen ES91009® and Paraloid B72® and of other coating systems containing corrosion inhibitors when applied by brushing or immersion methods on clean or corroded surfaces in a climatic cabinet. Poligen ES91009 was found to offer the best protection when applied by immersion (coatings of average thickness ~ 40 µm) on uniform, non-porous corroded surfaces. Degriigny [10], during the same research project, submitted the coated corroded coupons to a 12-month indoor exposure in museum environment with fluctuation in %RH levels and temperature. Again Poligen exhibited the best behaviour towards corrosion protection, while for Paraloid B72 coating slight edge defects were observed and a generally glossier effect.

One major disadvantage of all acrylic coatings -and Paraloid series in particular- is the lack of barrier properties. Therefore, their use for the protection of outdoor sculpture or architectural elements is limited or very short-term. The introduction of nano-alumina as a filler into acrylic coating systems was found to achieve better performance of coated surfaces of cultural heritage materials (ferrous and non-ferrous metals and marble), offering potentials of expanding use of the acrylic coatings in environmental applications. Previous studies [18]-[21] have reported aesthetic aspects and corrosion protection performance of Paraloid coating series (B72, B44, B67 plain and nano-Al₂O₃ enhanced) applied on Ag, Cu, and Al alloys. In a more recent laboratory study, Delagrammatikas et al. have investigated the effect of nano-Al₂O₃ concentration in various Paraloid B72 physicochemical properties related to coating application characteristics and behaviour towards UV ageing, wetting and water uptake during total immersion corrosion [22]. The addition of Al₂O₃ nano-powder between 1.5 and 2 % leads to optimum dispersion in polymer matrix and the coated surfaces exhibit maximum hydrophobicity -especially after exposure to sunlight at temperatures near glass transition temperature (T_g). For the same systems a minimum water uptake compared to plain Paraloid B72 and all the other tested syntheses was also observed [22].

Chiantore and Lazzari have evaluated the behaviour of acrylic and methacrylic resins towards photo-oxidation. Their experiments have concluded that Paraloid products, containing solely ethyl and methyl esters are stable under UV exposure, while resins which contain longer ester groups are more sensitive to photo-oxidation [23]. In other words, Paraloid B72 exhibits higher stability against UV ageing than Paraloids B66 and B67, but is less hydrophobic. This is why in most outdoor applications the usually preferred acrylic coatings are Paraloids B66 and B67. The chemical composition, metallurgical features, microstructure and long-term atmospheric corrosion of monument steel reinforcements and joints has been the subject of several case studies [24]-[27].

The metallurgical examination and post-assessment of corrosion and mechanical performance of iron and low carbon steel clamps and dowels (ancient and restoration materials) at the Acropolis monuments has been investigated by research groups in collaboration with the Acropolis Restoration Service [26]-[31].



Figure 1. Highlights from laboratory tests during Phase 1: (a) Coating application by brush on uncorroded flat steel specimens and (b) Colour measurements on coated aluminum specimens

3. MATERIALS AND METHODS

3.1. First experimental phase

The first experimental phase (Phase 1) of this project comprises preparation of samples, accelerated weathering at laboratory scale, measurement of properties with respect to weathering time and assessment of performance.

Seven (7) polymer coating systems (2 plain acrylic polymers: Paraloid B66 & Paraloid B67, 2 composite acrylic polymers with addition of nano-alumina: Paraloid B66 + 2 % nano- Al_2O_3 & Paraloid B67 + 2 % nano- Al_2O_3 , 2 aqueous polyethylene emulsions: Poligen CE12 & Poligen CE18 and 1 duplex system consisting of inner layer of acrylic polymer and an outer layer of 1 microcrystalline wax: Paraloid B48N/Cosmoloid H80) were applied by brush on uncorroded flat steel sheets. Acrylic polymers were first dissolved in analytical-grade acetone, as to avoid the presence of water. Two coating layers were applied, each consisting of horizontal and perpendicular brush strokes. The first layer was allowed to dry for a period of 24 ± 2 h before the application of the second layer. This ensured that the second layer would increase the thickness of the coating. Application method tried to maintain consistence with in-situ application conditions in a monument restoration site, such as the Acropolis of Athens, which is exposed to open air and where the application site is usually only accessible using scaffolding. Thus, application is only possible using a brush, as airbrush use would

be hindered by wind and immersion is not possible, while longer drying periods between the application of the different layers could not follow worksite schedule (Figure 1a). The coating systems composition and application characteristics are described in Table 1. A second set of the first phase coating was applied using the same methodology on aluminum coupons for the purpose of measuring physicochemical properties.

The coating thickness of the steel coupons was measured by the Eddy current technique using a (Elcometer 256F; ASTM E376) portable device (Table 1) and consequently were exposed to accelerated corrosion in a salt-spray chamber (Fogmaster Salt Spray; ASTM B117) for 4 h, using a 5 % w/w NaCl solution at 30 ± 5 °C. This exposure time was sufficient for corrosion initiation under non-barrier coatings, thus, allowing a comparative examination of the coatings' protective potential. Prior to exposure to the salt-spray testing apparatus, the coupons' periphery was masked by tape in order to avoid edge effects. Specimens were submitted to accelerated weathering 30 days after the application of the second layer of coating, as to allow for the evaporation of the solvent. After removing the specimens from the chamber, the surfaces were gently washed with de-ionized water and dried at ambient conditions.

The colour measurement was performed on the coated aluminum coupons in order to avoid any colour change due to base metal corrosion during weathering. The specimens were

Table 1. The coating systems tested in terms of corrosion protection, aesthetic aspects and hydrophobicity before and after weathering during the two phases of the project.

Coating	Substrate	Layer	Coating type	Solvent	Dry polymer to solvent ratio	Additive	Additive to dry polymer ratio	Thickness (μm)
<i>Phase 1 Laboratory Testing</i>								
SC_B66_10	Steel coupon	1 st & 2 nd	Paraloid B66®	Acetone	10 % w/v	-	-	3.0 ± 3.2
SC_B67_10	Steel coupon	1 st & 2 nd	Paraloid B67®	Acetone	10 % w/v	-	-	2.2 ± 0.6
SC_B66_10n2	Steel coupon	1 st & 2 nd	Paraloid B66®	Acetone	10 % w/v	nano Al_2O_3	2 % w/w	1.9 ± 0.3
SC_B67_10n2	Steel coupon	1 st & 2 nd	Paraloid B67®	Acetone	10 % w/v	nano Al_2O_3	2 % w/w	$3.3_{-0.4}$
SC_CE12	Steel coupon	1 st & 2 nd	Poligen CE12®	Water	as produced	-	-	10.7 ± 1.4
SC_CE18	Steel coupon	1 st & 2 nd	Poligen CE18®	Water	as produced	-	-	4.3 ± 0.5
SC_B48N/H80	Steel coupon	1 st	Paraloid B-48N®	Acetone	10 % w/v	-	-	26.0 ± 5.1
		2 nd	Cosmoloid H80®	-	-	-	-	
<i>Phase 2 In situ exposure</i>								
MP_B67_10n2	Steel joint	1 st & 2 nd	Paraloid B67®	Acetone	10 % w/v	nano Al_2O_3	2 % w/w	
MP_CE12	Steel joint	1 st & 2 nd	Poligen CE12®	Water	as produced	-	-	



Figure 2. Contact angle measurement of three best performing under UVB aging coatings. Measurements presented here were conducted on non-exposed specimens.

measured in CIE $L^*a^*b^*$ colour space (Figure 1b), using a portable spectrophotometer (Sheen Micromatch Plus; ASTM D1925, D2244) and Gloss was measured using a portable glossmeter (Sheen Tri-Glossmaster; ASTM D523, D2457). Hydrophobicity of the coatings' surface was measured by the contact angle method in a custom-made apparatus consisting of a LED light source, a frosted glass filter and a circular polarizer filter set in this order behind the specimen in order to provide uniform backlit, a horizontal specimen holder and a Canon 40D camera, equipped with a Canon EF 100 1:2.8 USM Macro Lens at 1:1 magnification setting and a circular polarizer filter. The main optical axis of the lens was set to form a 3° angle with the specimen surface. DI water droplets of a standard volume of $20 \mu\text{L}$ were placed on the coated surfaces by a dosimetric pipette. For each system, the contact angle was determined by an average of measurements on five different droplets (Figure 2).

Measurements were performed 30 days after the application of the second layer and consequently specimens were subjected to accelerated photo-oxidation in a QUV/spray, Q-panel Lab Products apparatus (ISO 11341, ASTM D 4587 and EN-ISO11507:1997), using UVB 313 lamp sources. The specimens underwent an initial 4 hour exposure in 100 % RH and a total of 52 repeated cycles (420 h). Each cycle corresponds to 4 h of UVB radiation at 50°C and high RH levels followed by 4 h of condensation (100 % RH at 40°C without radiation). At an interval of 216 h and at the end of the test, the specimens were measured using the same methodologies described above.

3.2. Second experimental phase

The second experimental phase (Phase 2) of this project comprises the application of two selected coatings (Table 1) on pre-corroded historic steel joints used by the Balanos restoration

works during the first half of the 20th century, which were removed and replaced by titanium joints during the current Acropolis restoration program. The historic restoration steel joints, used under the permission of the Acropolis Restoration Service, contain very low concentrations of carbon and other alloying elements and inclusions such as sulfur. Their chemical composition along with their mechanical properties (micro-hardness and tensile stress values), studied by the authors in previous work [26], are very close to the ones of the original ancient and other restoration clamps [27], [29], [31].

The coatings were applied using the same methodology described in Phase 1. Contrary to the steel coupons, the surface of specimens in the second phase was rough and the coating was applied on porous corrosion products and not on a metallic surface. Thus, coatings thickness was not always uniform. Parts of the steel joints were left uncovered on purpose in order to examine whether the application of the coatings would cause accelerated corrosion to parts of the joints that are inaccessible and cannot be covered. Fresh metallic surfaces at the areas where the specimens were cut, were masked using an elastomer sealant, in order to eliminate the effects of these areas to the evolution of the corrosion phenomena.

After allowing 30 days for the coatings to set and the solvent to evaporate, the specimens underwent orthophotographic documentation (Canon 40D camera, equipped with a Canon EF 100 1:2.8 USM Macro Lens at 1:1.5 magnification setting) and then were placed on a Pentelic marble bottomed tray and exposed to atmospheric conditions and sunlight in situ on the Acropolis of Athens hill (Figure 3).

When the specimens completed a full year of exposure in environmental conditions (environmental temperature in Athens typically varies from -5°C to 45°C , sunlight, rain, snow and frost, as well as airborne particulates) the specimens were returned to the laboratory for assessment of the coatings' performance. The specimens' surface was once more documented using orthophotography under the same settings and illumination conditions as before exposure. Then the coatings were removed by the application of cotton swabs dipped in acetone and in some cases by glass fiber brush, as would be done when removing a coating in-situ.



Figure 3. The coated steel joints placed in a marble bottomed open case during field exposure near the monument.

Table 2. Effect of UV induced photo-oxidation on the properties of the coatings. Contact angle of water droplet is indicative of changes in hydrophobicity; Gloss is measured in arbitrary Gloss Units; Colour changes are calculated in CIE L*a*b* colour space, ΔL indicates changes in luminosity, Δa^* indicates changes between red (+) and green (-), while Δb^* indicates changes between yellow (+) and blue (-).

Coating System	Contact Angle (°- degrees)			Gloss (GU)		Colour Change after 420 h UV		
	0 h UV	216 h UV	420 h UV	0 h UV	420 h UV	ΔL^*	Δa^*	Δb^*
Poligen CE12	88 ± 5	80.8 ± 1.6	78 ± 3	85.7	82.7	-6.7	-17.6	3.9
Poligen CE18	62 ± 13	80 ± 11	81 ± 4	100.2	11.0	3.6	8.2	27.3
Paraloid B66	87 ± 3	80 ± 4	75.0 ± 0.6	136.1	120.0	0.2	2.9	8
Paraloid B67	89 ± 3	80.4 ± 0.6	75.0 ± 2.3	92.9	52.6	-0.6	-12.5	5.9
Paraloid B67 + 2 % nano Al ₂ O ₃	88 ± 4	80.6 ± 2.0	76.6 ± 1.4	82.5	72.2	-0.6	17.6	4.1
Paraloid B66 + 2 % nano Al ₂ O ₃	82.8 ± 1.4	80.2 ± 2.2	77.8 ± 2.1	125.0	120.1	-2.2	8.7	8
Paraloid B48 + Cosmoloid H80	114 ± 6	100 ± 5	100 ± 3	4.2	6.1	-6.7	-17.6	-7.6

The reversibility of the coatings, after one year of exposure, was documented by means of Raman spectroscopy, using a Renishaw In Via dispersive Raman apparatus, using a 532 nm solid state laser (green) as excitation source. The laser beam power was set at 0.5-1 %. For each spectrum collection 3 accumulations and 20 s exposure time were applied. The measurement areas on the sample surface were specified using a x20 objective lens.

Raman spectra allowed the identification of corrosion products and drawing of conclusions on the stability of the corrosion layers. Raman spectra were collected from exposed coated areas, after the coating was removed by solvent and/or glass-fiber brush, as well as from samples of the coatings applied on glass.

4. RESULTS AND DISCUSSION

4.1. First experimental phase

The acrylic polymers (Paraloids with and without nano-alumina) were less viscous, and thus were easily applied by brush creating uniform coating films of low average thickness (below 5 μm). The aqueous wax emulsions (Poligen products) were also easily workable and the final coatings were uniform and generally thicker (especially Poligen CE12 with average thickness of 10.7 ± 1.4 μm). The duplex layer (Paraloid B48N + Cosmoloid H80) exhibited the highest thickness (26 ± 5 μm), but the coating was irregular because of the low workability of micro-crystalline wax during application of the outer layer. The micro-crystalline wax Cosmoloid H80 exhibited low workability and led to non-uniform layer thickness and not acceptable aesthetic result.

The as-applied coating systems exhibit satisfactory initial hydrophobic behaviour (values ranging from 83° up to 114°) (Table 2). In case of Poligen CE18, the particularly low contact angle values are not acceptable. The highest hydrophobic properties are observed for the duplex acrylic/microcrystalline wax system. Comparison of contact angle values, measured at 216 h and 420 h intervals of UV-ageing, with the initial values of polymer coatings reveals a gradual decrease for almost all coatings. This alteration corresponds to a decrease of hydrophobicity and is also characteristic of microstructural changes of polymeric materials. On the contrary, in case of Poligen CE18 the sharp increase in contact angle that took place

within the first 216 hours could be attributed to cross-linking effects.

The highest gloss values were observed in the cases of Paraloid B66 and Poligen CE18 coated surfaces (Table 2). Paraloid B67 and Poligen CE 12 create a relatively matte finish and the duplex coating exhibits the lowest gloss value. The addition of nano-alumina generally tends to decrease the gloss effect, which is a desirable effect. After the exposure to UV/condensation cycles a slight decrease in gloss is observed for all coating systems, except for Poligen CE 18 where a significant alteration took place (a drop from 100.2 to 11.0 GU).

The impact of UV-ageing is also evident by the variation of colour component values (Table 2). The main finding is a general trend towards the increase of b^* values (yellowing effect). No specific pattern can be deduced for parameter a^* . Besides yellowing, no other conclusions may be drawn from colour measurements, as the coatings are transparent, and the effect of the background cannot be ignored. Poligen CE 18 has undergone extensive yellowing, which can be assessed even macroscopically. Poligen CE18 exhibited intense yellowing and increase of contact angle (increase of hydrophobicity), which could be related to polymer constituents cross-linking. The nano-alumina enhanced acrylic polymers have also increased their b^* values. Less affected were the plain Paraloid coatings and Poligen CE 12, where no visible alteration could be observed.

In general, the performance of all acrylic coatings and of Poligen CE12 wax against UV induced colour/gloss and hydrophobicity changes was regarded as satisfactory. In most cases, slight colour and gloss changes were observed. A general trend towards yellowing, less glossy appearance and higher susceptibility to wetting with the increase of UV exposure time can be deduced.

Macroscopic evaluation of the salt-spray exposed steel specimens demonstrated that the best behaviour was exhibited by Poligen CE12 coatings. The Paraloid B67 + 2 % nano-alumina coated specimens also exhibited very good corrosion resistance (Figure 4).

Concluding the 1st experimental phase, Paraloid B67 + 2 % nano alumina and Poligen CE12 were chosen for proceeding with the second experimental phase. The selection was based both on the performance of the two materials and on the fact that they represent the two different coating categories tested, i.e. acrylic resins and waxes.

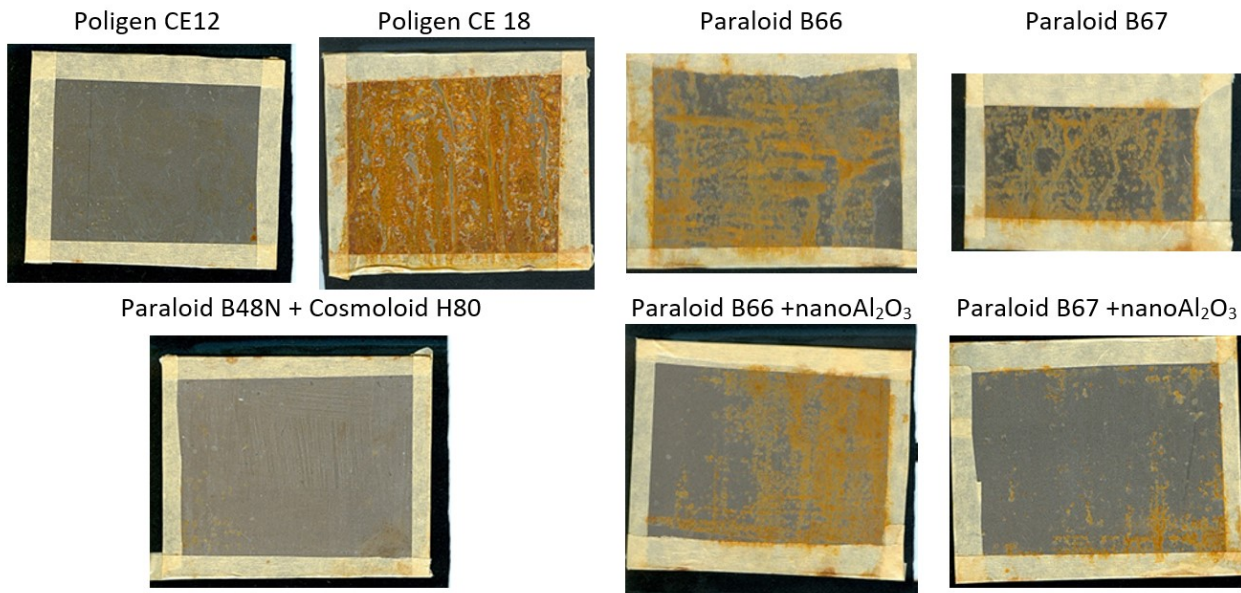


Figure 4. Macroscopic documentation of coated steel specimens after 4 h of exposure in 5 % NaCl salt-spray chamber

4.2. Second experimental phase

Application by brush of the two coatings over the pre-corroded, rough and porous surface of the historic steel joints revealed a very different behaviour between the two selected materials. Contrary to the perfect application of Poligen CE12 over metal coupons during Phase 1 and bibliographic data for application by immersion of this coating over slightly pre-corroded coupons, which provided excellent results [17], application by brush was not easy, the coating material could not permeate and wet the porous surface, resulting to trapping of air and a non-uniform layer produced. This may be attributed to the higher viscosity of the product as well as to the surface tension of the suspension which prohibit wetting of the corroded

surface. On the other hand, Paraloid B67 + 2 % nano- Al_2O_3 application by brush was very smooth and easy. The coating material wetted the surface and penetrated in the pores, acting both as coating and a consolidating material.

The dried acrylic coatings (Paraloid B67 + 2 % nano- Al_2O_3) achieved good adhesion and uniform covering of porous corrosion products. The dry wax emulsion (Poligen CE12) after the evaporation of the liquid phase, produced a less uniform result, exhibiting shrinkage, local detachments and micro-cracks. These morphological features suggest an early initiation of exfoliation.

Figure 5 and Figure 6 present the orthophotographic documentation of the historic steel joints during all stages of

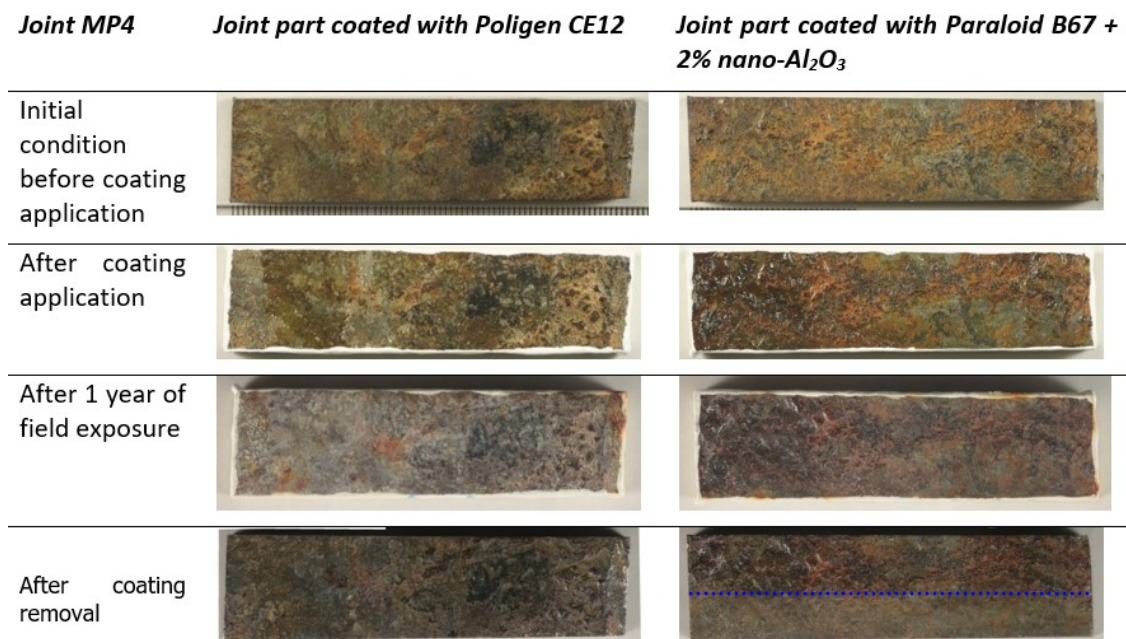


Figure 5. Photographic documentation of joint MP4 before and after the coating systems application and after the coatings removal. Poligen CE12 was removed using a glass fiber brush, while Paraloid B67 based coating was removed using acetone on cotton swabs. The area below the dotted blue line was treated at second stage of Paraloid coating removal with a glass fiber brush. The length of the specimen is about 7.3 cm.

Joint MP169

Joint part coated with Poligen CE12

**Joint part coated with Paraloid B67 +
2% nano- Al_2O_3**

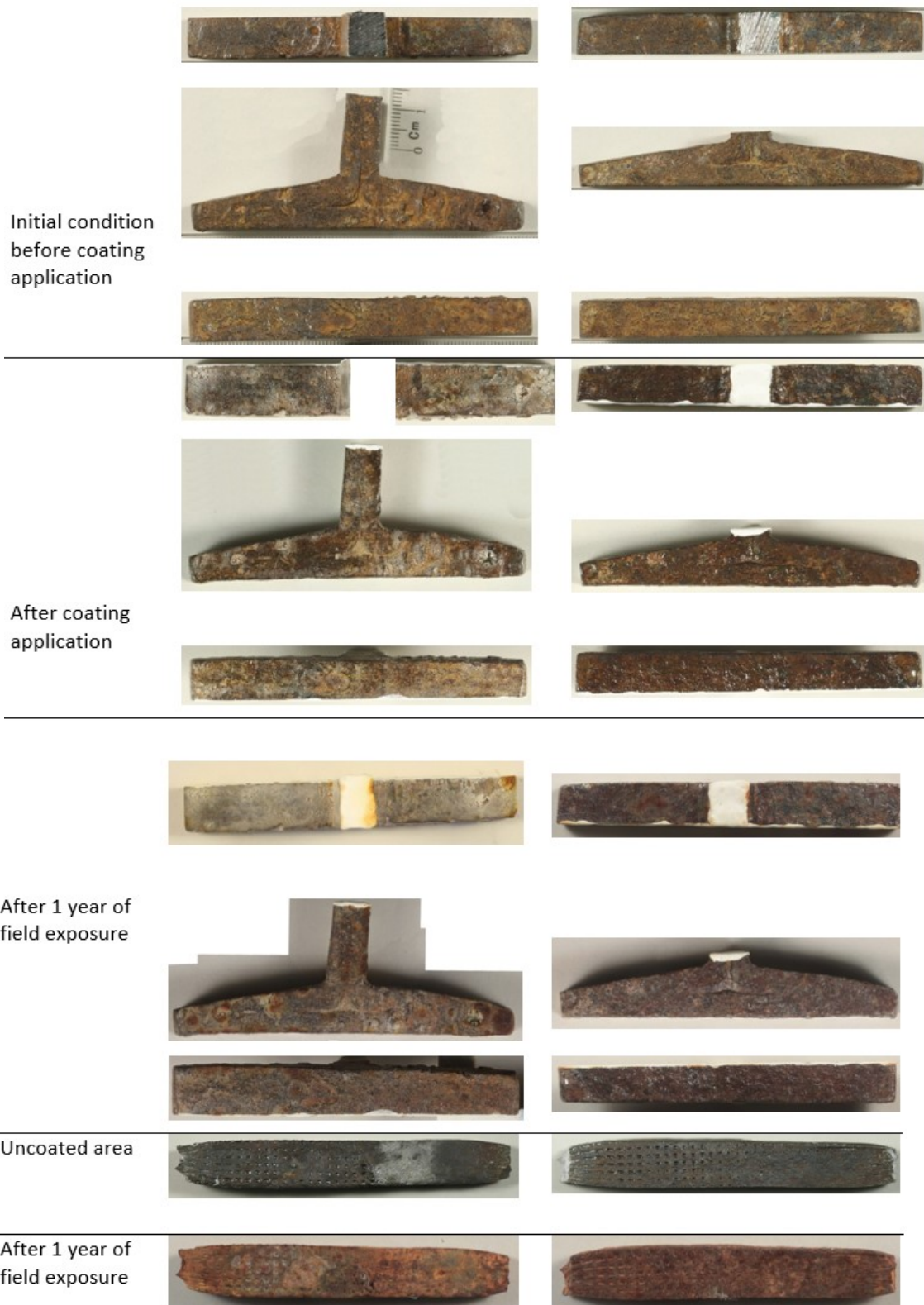


Figure 6. Photographic documentation of joint MP169 (coated and uncoated) at various intervals before and after the coating systems application and after 1 year of field exposure. The uncoated specimen has been significantly more corroded than both coated specimens. The average thickness of the clamp's shaft is 9 mm.

Phase 2 experiments. A direct comparison with uncoated clamp surfaces is also provided. The macroscopic assessment of Paraloid B67+2 % nano- Al_2O_3 post-exposure surface condition gave acceptable results and no indications of serious failure. The same result was obtained by the application of Poligen CE12 over compact and relatively non-porous corrosion products. In areas where corrosion products were rougher Poligen CE12 did not maintain contact with the substrate and was washed away. The areas which remained covered by the protective coatings present a better conservation condition, while in the areas that were left blank corrosion was not inhibited. In none of the blank areas or the areas that Poligen CE12 was washed away did corrosion phenomena appeared more severe than in the specimen that was left uncoated.

Raman vibrational spectroscopy was used in order to detect polymer degradation effects and chemical alteration of rust scales.

On uncoated blank surfaces of the clamps, mixtures of Fe oxy-hydroxides and oxides were detected on the surface of rust scales. The predominant oxy-hydroxide compound, detected in all collected spectra, was lepidocrocite ($\gamma\text{-FeOOH}$), with Raman peaks at 244-249 cm^{-1} , 300-305 cm^{-1} , 366-374 cm^{-1} , 520 cm^{-1} , 632-670 cm^{-1} , 1036-1047 cm^{-1} and 1297-1309 cm^{-1} [4], [32], [33], [34], [35], [36]. One representative spectrum of the corroded clamp surfaces is curve (c) presented in Figure 7. Some noticeable deviations between lepidocrocite peaks reported by this work and Raman data references corresponding to well crystallized compounds - and of course differences among several literature sources- can be attributed to the wide range of crystallinity of these compounds. In some cases the iron oxy-hydroxides are of amorphous nature.

It is worth commenting on some more rare detections observed locally on blank specimen areas: the weak broad shoulders within the range 1036-1115 cm^{-1} could be attributed to

a mixture of lepidocrocite ($\gamma\text{-FeOOH}$) with goethite ($\alpha\text{-FeOOH}$) [4], [35]. Some oxides were also identified. The presence of peaks at 403-413 cm^{-1} could be related to hematite ($\alpha\text{-Fe}_2\text{O}_3$) [37], [38], [39] and the vibration at 721 cm^{-1} is a possible match with maghemite ($\gamma\text{-Fe}_2\text{O}_3$) [37], [40], [41] or the chloride-containing Fe(III) oxy-hydroxide known as akaganeite [34], [40], [41]. A twin peak constituted of two components at 674 cm^{-1} and 721 cm^{-1} indicates the presence of maghemite [4], [40]. The relevant spectra are not presented for brevity reasons.

Optical Microscope images acquired during Raman Spectroscopy show the areas where the exposed coated specimens were analysed (Figure 8). On Paraloid B67+2 % nano- Al_2O_3 coated surfaces, the vibrations at 250 cm^{-1} , 521 cm^{-1} , 637 cm^{-1} and 1291 cm^{-1} of Figure 9(a) were attributed to lepidocrocite ($\gamma\text{-FeOOH}$) and the ones observed at 383 and 294 cm^{-1} to goethite ($\alpha\text{-FeOOH}$) [4], [32], [33]. The group of vibration peaks at 2876 cm^{-1} (symmetric CH_2 stretching), 2926 cm^{-1} and 2960 cm^{-1} (symmetric CH_3 stretching) match with reference spectra of poly- isobutyl methacrylate [42], [43]. The band at 1442 cm^{-1} also is related to asymmetric CH_3 bending of polymer molecules [42].

On Poligen CE12 coated surfaces, the spectra presented in Figure 10(a) exhibit Raman peaks at 250 and 1292 cm^{-1} , which indicate the presence of lepidocrocite [4], [32], [33]. The peak at 541 cm^{-1} corresponds to magnetite (Fe_3O_4) [44], [39], while the one at 374 cm^{-1} could be attributed to lepidocrocite [4], [32], [34] and/or ferrihydrite ($\text{Fe}_5\text{HO}_8\cdot 4\text{H}_2\text{O}$) [4], [40]. The band at 638 cm^{-1} does not match with any of the typical Fe oxides or oxy-hydroxides and could be related to amorphous or low crystallinity $\gamma\text{-FeOOH}$. The characteristic vibrations at 2845, 2881 and 2943 cm^{-1} and most probably the weak peak at 1431 cm^{-1} are attributed to the constituents of Poligen CE12: poly (vinyl stearate), polyethylene and poly (propyl acrylate). Unfortunately, no specific literature reference on vibrational

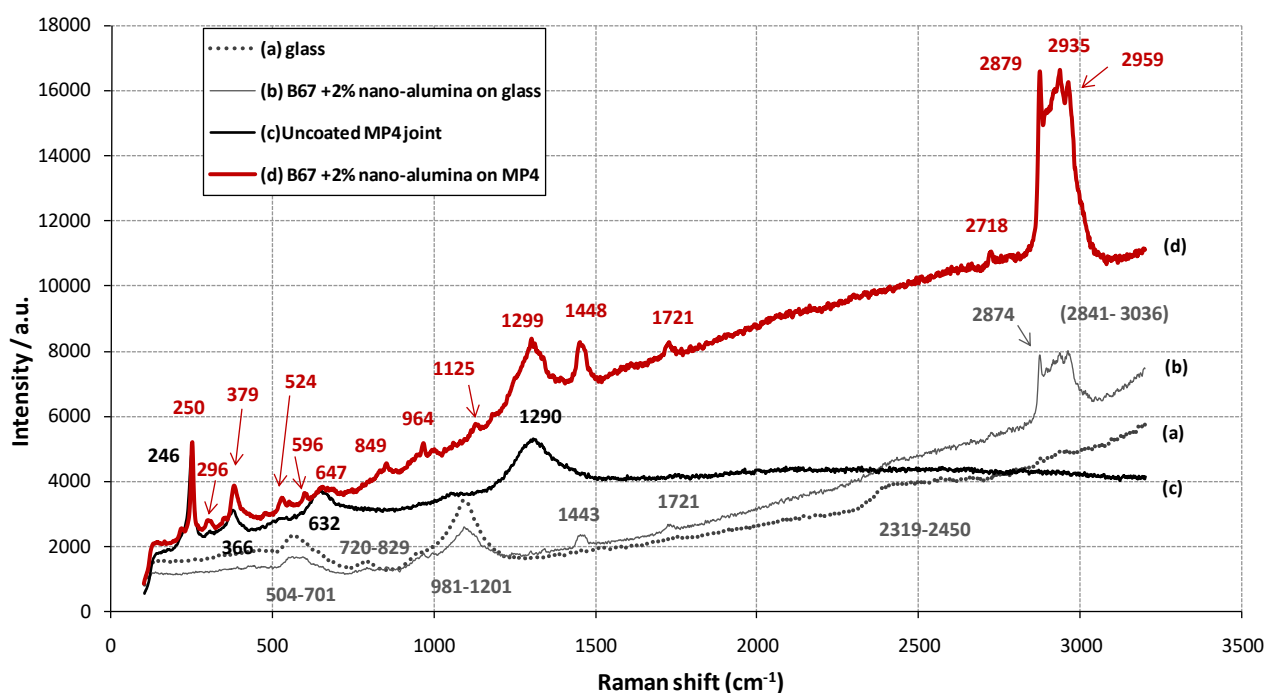


Figure 7. Representative Raman spectra of surfaces coated with Paraloid B67 + 2 % nano- Al_2O_3 - The four analysed surfaces correspond to: (a) glass substrate, (b) glass coated with Paraloid B67 + 2 % nano- Al_2O_3 , (c) corroded MP4 steel joint and (d) corroded steel joint MP4 coated with Paraloid B67 + 2 % nano- Al_2O_3 after 1 year of field exposure.

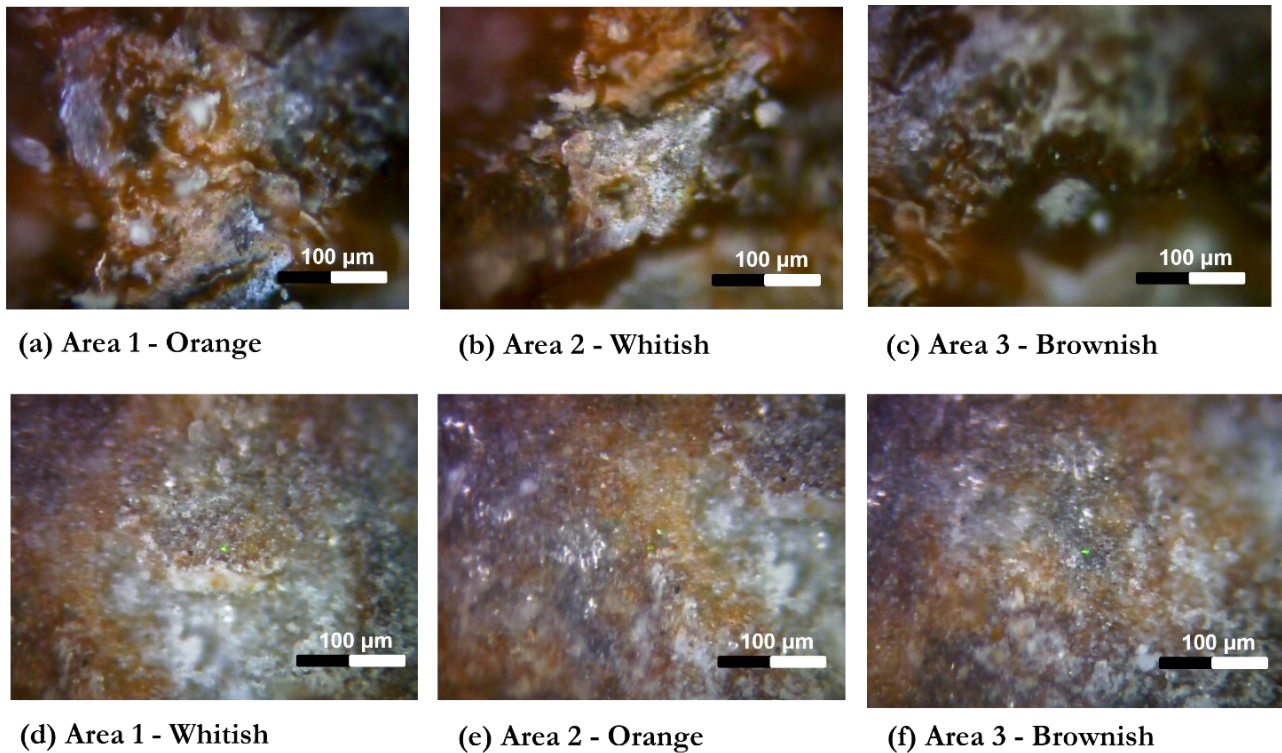


Figure 8. Stereoscopic images (x20) of the analysed areas on coated parts of MP4 steel joint, after 1 year of field exposure. The photographs of Paraloid B67 +2 % nano- Al_2O_3 coated areas (a)-(c) correspond to spectra of Figure 9(a) and the photographs of Poligen CE12 coated areas (d)-(f) correspond to spectra of Figure 10(a).

patterns of Poligen products could be found. Since the particular product is a wax emulsion, some useful correlations can be made with Raman data reported for paraffin waxes: Peaks within the range of $2848\text{--}2882\text{ cm}^{-1}$ have been reported for industrial paraffin waxes and carnauba waxes [45]. The peak at 2845 cm^{-1} is a CH_2 symmetrical stretching mode and the one at 2881 cm^{-1} is a CH_2 asymmetrical stretching mode. The shoulder observed at 2943 cm^{-1} could be a symmetric CH_3 stretching. Finally, the peak at 1431 cm^{-1} is most probably a CH_2 asymmetric bending mode [45].

Raman spectroscopy was used to determine the sufficient removal of the coatings and to assess the corrosion products under the removed coatings. The comparative Raman spectra before and after the coating removal are given in Figure 9(b) and Figure 10(b). The absence of polymer-related vibrations confirms the efficient coating removal in both cases.

Regarding the chemical species of corrosion products, some crucial findings indicate different corrosion protection features for the two tested coatings. In the case of Paraloid B67 +2 % nano-alumina coated areas, after the chemical and mechanical removal (combination of acetone swabbing and mechanical cleaning by glass fiber brush), the detected lepidocrocite peaks at 250 cm^{-1} , 377 cm^{-1} and 1296 cm^{-1} [4], [32] were weaker, the goethite peak at 294 cm^{-1} [4], [32], [33] remained the same and an additional vibration at 664 cm^{-1} was related to magnetite [34], [37], [39], [40] (Figure 9(b)). These results are consistent with the assumption that some loose superficial $\gamma\text{-FeOOH}$ compounds were removed together with the polymer layer. No significant chemical changes were observed due to seasonal wet/dry cycles during the field testing.

In the case of Poligen CE12 coated areas, after the mechanical removal by glass fiber brush, the main lepidocrocite peaks at

about 250 cm^{-1} and $1290\text{--}1300\text{ cm}^{-1}$ were not detectable. The peaks observed around $302\text{--}304\text{ cm}^{-1}$, 388 cm^{-1} and 418 cm^{-1} are attributed to goethite [4], [5], [32], [33], [39]. The spectrum acquired from a crust extrusion (Figure 10(b), relief) revealed a strong peak at 674 cm^{-1} could be related to either magnetite [34], [37], [44] or poorly crystallized ferroxhyte ($\delta\text{-FeOOH}$) [4] and a weaker at 548 cm^{-1} that matches magnetite [34], [39]. The spectrum acquired from a crust cavity (Figure 10(b), center) exhibited a peak at 694 cm^{-1} which indicates the formation of ferroxhyte ($\delta\text{-FeOOH}$) [4] or/and ferrihydrite ($\text{Fe}_5\text{HO}_8\cdot 4\text{H}_2\text{O}$) [4], [5]. Another peak at 473 cm^{-1} could be attributed to maghemite ($\gamma\text{-Fe}_2\text{O}_3$) or wüstite (FeO) [40].

According to models of long-term natural atmospheric corrosion, goethite, as well as magnetite, is usually encountered in the inner layer of rust scales and has isolating behaviour, while lepidocrocite is the predominant active phase in superficial layers [1], [3], [4]. The evolution of poorly crystallized ferroxhyte ($\delta\text{-FeOOH}$) and ferrihydrite ($\text{Fe}_5\text{HO}_8\cdot 4\text{H}_2\text{O}$) has been reported by Monnier et al. as constituent of rust layers grown on ferrous medieval reinforcements [5]. These low crystallinity products are believed to act as electrochemically reactive phases inside the corrosion crust during atmospheric exposure [5]. Thus, the evolution of the particular corrosion species on surfaces after the removal of Poligen polymer, testifies sites of active electrochemical corrosion inside the corrosion crust. The mechanical cleaning by brush, apart from removing the polymer coating also removed the outer lepidocrocite phase and revealed layers of goethite, magnetite and ferroxhyte/ ferrihydrite. The chemical variations observed at sites of different texture, and more specifically the identification of electrochemically reactive species inside corrosion crust cavities indicate the local acceleration of corrosion reactions.

Overall, it can be deduced that joint areas coated with Paraloid B67 enhanced with 2 % nano-alumina offered better corrosion protection during field exposure. Moreover, the dispersed nano-powder in the acrylic polymer matrix seems to play a significant role in filling the porosity of rust scales, at least to some degree.

5. CONCLUSIONS

The assessment of 7 coating system properties and performance during laboratory testing of Phase 1 led to the selection of Poligen CE12 (aqueous emulsion of polyethylene wax) and Paraloid B67 + 2 % nano- Al_2O_3 acrylic coating as the most suitable materials to be used in the next phase of the steel joint conservation project. Both coatings exhibited very satisfactory behaviour concerning application convenience, corrosion protection of steel substrate, physicochemical stability against weathering (UV and wetting) when applied on uncorroded smooth metallic substrates.

Results of Phase 2 lead to some very interesting conclusions:

- Both Poligen CE12 and Paraloid B67+2% nano- Al_2O_3 were proved to be two fully reversible conservation materials for corroded steel parts.
- Poligen CE12, despite its good performance on clean flat metal specimens, did not exhibit the same adhesion and uniform wetting properties when applied on porous and coarse corroded surfaces and in many local defects were observed after coating drying.

- Paraloid B67 + 2 % nano- Al_2O_3 coating application was uniform and the dry coatings elaborated good adhesion and coverage of the local surface porosity and roughness.
- The Paraloid B67+2 % nano- Al_2O_3 composite acrylic coating also offered better corrosion protection during the 1-year atmospheric field exposure in the monument site and was therefore proposed as the most suitable conservation material for the protection and consolidation of Erechtheion steel joints that are not directly exposed to rainfall and drainage areas.
- The sealing properties of Poligen CE12 exhibited during Phase 1 and the excellent application characteristics of Paraloid B67+2 % nano- Al_2O_3 lead to the proposal of testing a new duplex coating system consisting of an inner Paraloid B67+2 % nano- Al_2O_3 layer in contact with the corrosion products and a second Poligen CE12 layer in contact with the atmosphere. This duplex coating needs to be experimentally tested before it is proposed for application.

ACKNOWLEDGEMENT

The authors express their gratitude to the Committee for the Conservation of the Acropolis Monuments (ESMA), as well as to the Acropolis Restoration Service (YSMA) for their approval in the use of the joints from the earlier restoration project of Balanos. Special acknowledgement and gratitude are to Prof. V.

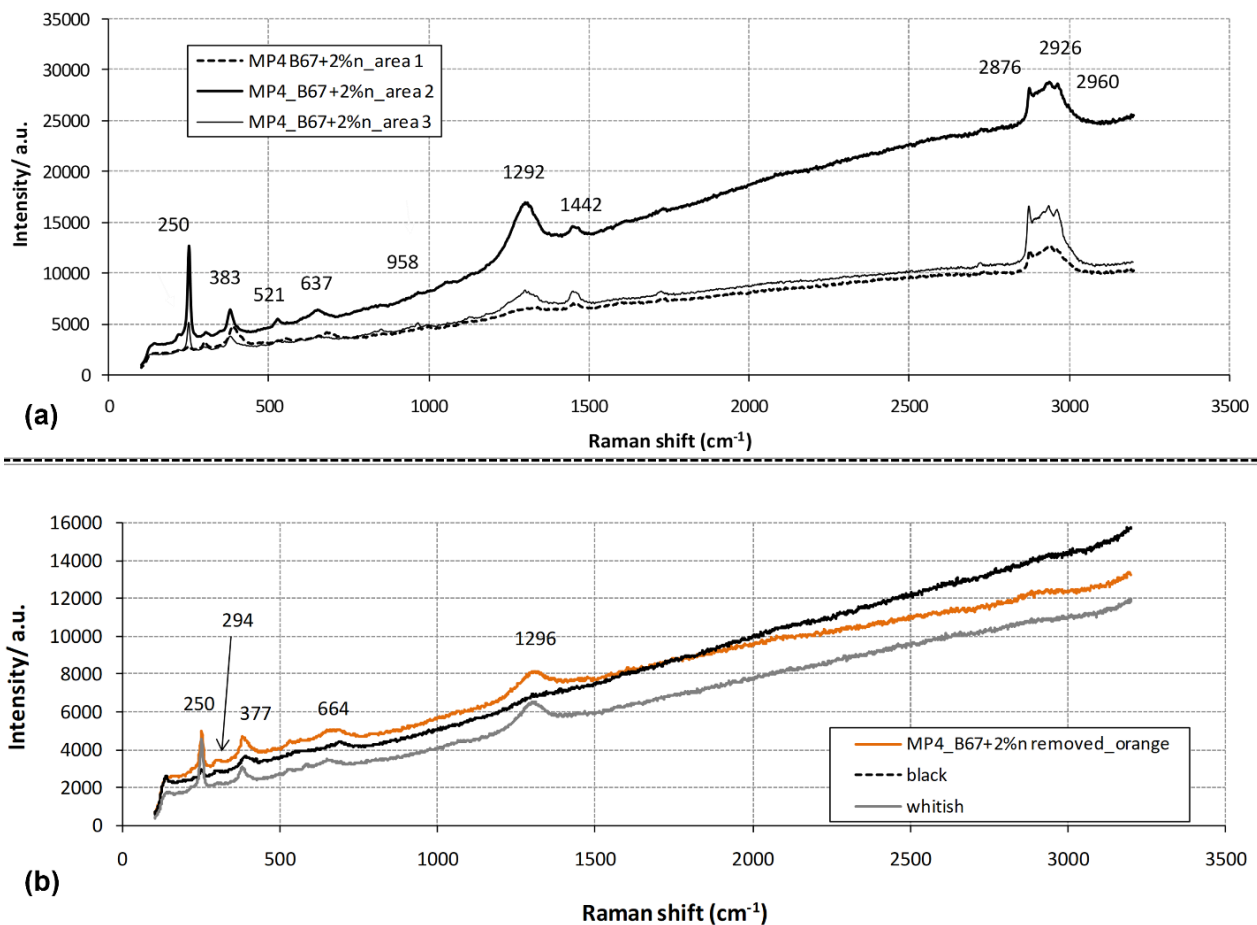


Figure 9. Characteristic Raman vibrations of Paraloid B67 + 2 % nano- Al_2O_3 polymer and corrosion products detected after 1 year of field exposure on (a) coated areas of MP4 joint and (b) the same areas after coating removal (swabbing with acetone and brushing with a glass brush).

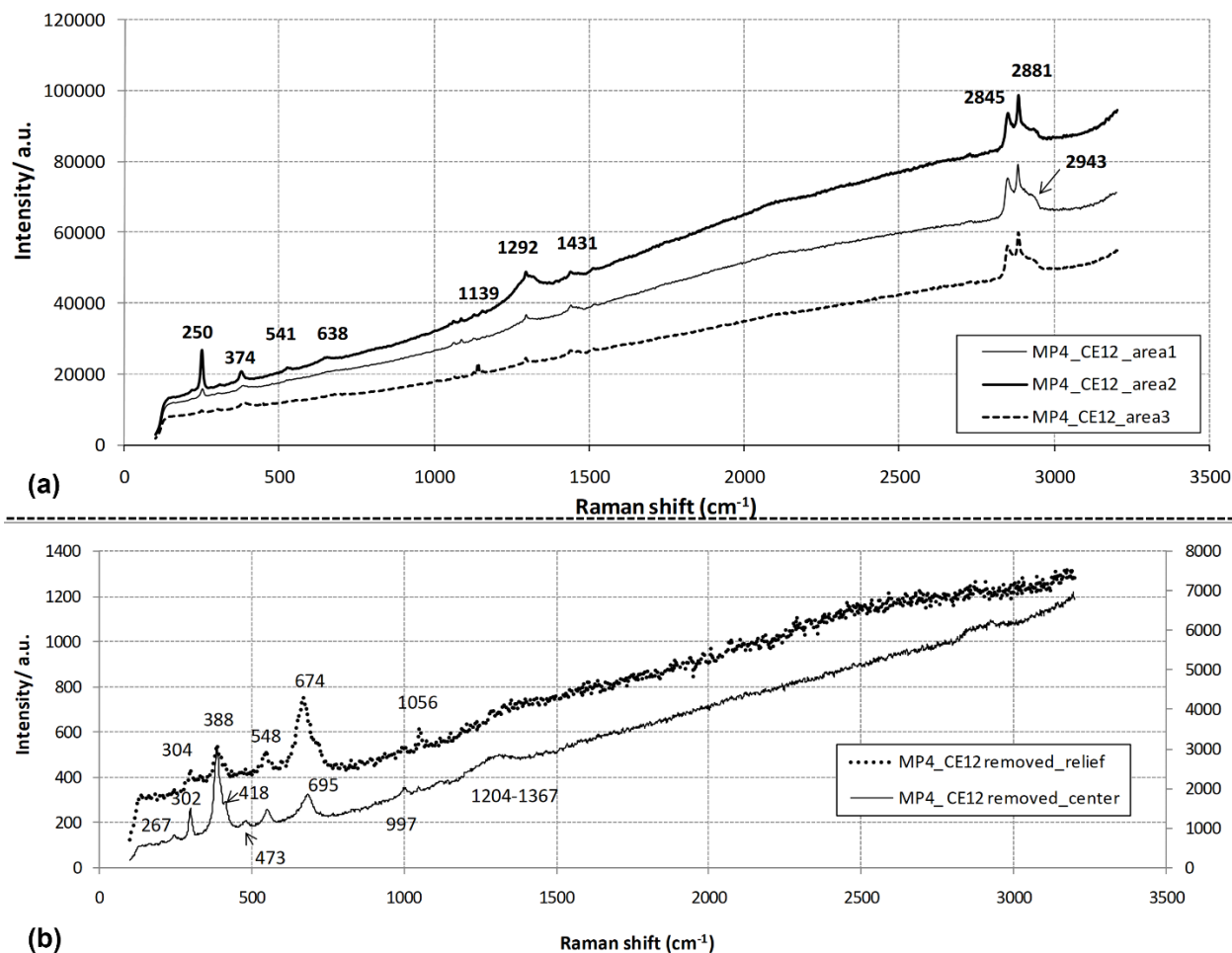


Figure 10. Characteristic Raman vibrations of Poligen CE12 polymer and corrosion products detected after 1 year of field exposure on (a) coated areas of MP4 joint and (b) the same areas after coating removal (brushing with a glass brush)

Kaselouri-Rigopoulou, member of ESMA for her contribution and scientific support

The authors would also like to thank Dr. P. Gyftoy and Prof. E. Pavlatou (Department of Chemical Sciences/ School of Chemical Engineering) in acknowledgement to their technical assistance regarding spectroscopic measurements and for the operation of the Raman microscope.

REFERENCES

- [1] D. Neff, S. Reguer, L. Bellot-Gurlet, P. Dillmann, R. Bertholon, Structural characterisation of corrosion products on archaeological iron. An integrated analytical approach to establish corrosion forms, *J. Raman Spectrosc.* 35 (8-9) (2004) pp. 739-745. DOI: [10.1002/jrs.1130](https://doi.org/10.1002/jrs.1130)
- [2] M. Saheb, D. Neff, P. Dillmann, M. Descostes, H. Matthiesen, Long-term anoxic corrosion of iron, in: *Corrosion and Conservation of Cultural Heritage Metallic Artefacts*. P. Dillmann, D. Watkinson, E. Angelini, A. Adriaens (editors). Woodhead Publishing, Oxford, Cambridge, Philadelphia, New Delhi, 2013, ISBN 978-1-78242-154-2, pp.260-284.
- [3] P. Dillmann, F. Mazaudier, S. Hœrlé, Advances in understanding atmospheric corrosion of iron. I. Rust characterisation of ancient ferrous artefacts exposed to indoor atmospheric corrosion, *Corros. Sci.* 46 (2004) pp. 1401-1429. DOI: [10.1016/j.corosci.2003.09.027](https://doi.org/10.1016/j.corosci.2003.09.027)
- [4] D. Neff, L. Bellot-Gurlet, Ph. Dillmann, S. Reguer, L. Legrand (2006), Raman imaging of ancient rust scales on archaeological iron artefacts for long-term atmospheric corrosion mechanisms study, *J. Raman Spectrosc.*, 37, pp. 1228–1237. DOI: [10.1002/jrs.1581](https://doi.org/10.1002/jrs.1581)
- [5] J. Monnier, E. Burger, P. Berger, D. Neff, I. Guillot, P. Dillmann, Localisation of oxygen reduction sites in the case of iron long term atmospheric corrosion, *Corros. Sci.* 53 (2011) pp. 2468–2473. DOI: [10.1016/j.corosci.2011.04.002](https://doi.org/10.1016/j.corosci.2011.04.002)
- [6] M. Morcillo, I. Díaz, H. Cano, B. Chico, D. de la Fuente, Atmospheric corrosion of weathering steels. Overview for engineers. Part I: Basic concepts, *Constr. Build. Mater.* 213 (2019) pp.723–737. DOI: [10.1016/j.conbuildmat.2019.03.334](https://doi.org/10.1016/j.conbuildmat.2019.03.334)
- [7] S. Hœrlé, F. Mazaudier, Ph. Dillmann, G. Santarini, Advances in understanding atmospheric corrosion of iron. II. Mechanistic modelling of wet–dry cycles, *Corros. Sci.* 46 (2004) pp. 1431-1465. DOI: [10.1016/j.corosci.2003.09.028](https://doi.org/10.1016/j.corosci.2003.09.028)
- [8] Watkinson, David. Preservation of metallic cultural heritage. in: *Shreir's Corrosion*. R. A. Cottis (editor). 4th ed., Vol. 4. Elsevier, London, 2010, ISBN 9780444527882. pp. 3307-3340.
- [9] A. Artesani, F. Di Turo, M. Zucchelli, A. Traviglia, Recent Advances in Protective Coatings for Cultural Heritage - An Overview, *Coatings* 10 (2020) 217. DOI: [10.3390/coatings10030217](https://doi.org/10.3390/coatings10030217)
- [10] C. Degrygn, The search for new and safe materials for protecting metal objects, in: *Metals and Museums in the Mediterranean - Protecting, Preserving and Interpreting*. V. Argyropoulos (editor). TEI of Athens, ISBN 978-960-87753-8-1, pp.179 -231.

- [11] C. V. Horie, *Materials for conservation- organic consolidants, adhesives and coatings*, Butterworth & Heinemann, London, 1987, ISBN 978-0-408-01531-8
- [12] V. Argyropoulos, M. Giannoulaki, G. P. Michalakakos, A. Siatou, A survey of the types of corrosion inhibitors and protective coatings used for the conservation of metal objects from museum collections in the Mediterranean basin, in: *Strategies for Saving our Cultural Heritage, Proceedings of International Conference on Conservation Strategies for Saving Indoor Metallic Collections with a Satellite Meeting on Legal Issues in the Conservation of Cultural Heritage*, V. Argyropoulos, A. Hein and M. A. Hatith (editor.). TEI of Athens, 2007, ISBN 978-960-87753-7-4, pp. 166-170.
- [13] Y. Shashoua, T. Holst, H. Matthiesen, Matching surface treatments to display environments for industrial objects, Department of Conservation, National Museum of Denmark, ZENODO (2010) pp 1-30.
DOI: [10.5281/zenodo.4086680](https://doi.org/10.5281/zenodo.4086680)
- [14] A. Siatou, V. Argyropoulos, D. Charalambous, K. Polikreti, A. Kaminari, Testing new coatings systems for the protection of metal collections exposed in uncontrolled museum environment, Proc. of the International Conference on Strategies for Saving Indoor Metallic Collections with a Satellite Meeting on Legal Issues in the Conservation of Cultural Heritage, Cairo, 25 February - 1 March 2007.
DOI: [10.1002/app.46011](https://doi.org/10.1002/app.46011)
- [15] B. Salvadori, A. Cagnini, M. Galeotti, S. Porcinai, S. Goidanich, A. Vicenzo, C. Celi, P. Frediani, L. Rosi, M. Frediani, G. Giuntoli, L. Brambilla, R. Beltrami, S. Trasatti, Traditional and innovative protective coatings for outdoor bronze: Application and performance comparison, *J. Appl. Polym. Sci.* 135 (2018) 46011.
DOI: [10.1002/app.46011](https://doi.org/10.1002/app.46011)
- [16] N. Swartz, T. Lassetter Clare, On the protective nature of wax coatings for culturally significant outdoor metalworks: Microstructural flaws, oxidative changes, and barrier properties, *JAIC*, 54:3 (2015) pp. 181-201.
DOI: [10.1179/1945233015Y.0000000012](https://doi.org/10.1179/1945233015Y.0000000012)
- [17] E. Cano, D. M. Bastidas, V. Argyropoulos, S. Fajardo, A. Siatou, J. M. Bastidas, C. Degriigny, Electrochemical characterization of organic coatings for protection of historic steel artefacts, *J. Solid State Electrochem.* 14 (2010) pp. 453-463.
DOI: [10.1007/s10008-009-0907-1](https://doi.org/10.1007/s10008-009-0907-1)
- [18] P. Vassiliou, J. Novakovic, K. Samara, Copper alloys and silver artefacts, protection by coatings with nano-alumina pigments, in: *Strategies for Saving our Cultural Heritage, Proceedings of International Conference on Conservation Strategies for Saving Indoor Metallic Collections with a Satellite Meeting on Legal Issues in the Conservation of Cultural Heritage*. V. Argyropoulos, A. Hein and M. A. Harith (editors). TEI of Athens, 2007, ISBN 978-960-87753-7-4, pp 132-137.
- [19] P. Vassiliou, V. Gouda, Ancient silver artefacts: Corrosion processes and preservation strategies, in: *Corrosion and Conservation of Cultural Heritage Metallic Artefacts*. P. Dillmann, D. Watkinson, E. Angelini, A. Adriaens (editors). Woodhead Publishing, Oxford, Cambridge, Philadelphia, New Delhi, 2013, ISBN 978-1-78242-154-2 pp. 213-235.
DOI: <https://doi.org/10.1533/9781782421573.3.213>
- [20] J. Novakovic, E. Georgiza, P. Vassiliou, V. Gouda, Degradation of Nano-alumina Acrylic Coatings on Silver, Proc. of the 19th International Corrosion Congress, Jeju, Korea, 2-6 November 2014.
- [21] O. Papadopoulou, H. Retsa, P. Vassiliou, V. Gouda, Protection of aluminium industrial heritage in a coastal environment with Paraloid coatings – A preliminary laboratory testing, Proc. of the 5th International Conference on Corrosion Mitigation and Surface Protection Technologies, Luxor, Egypt, 12- 15 December 2016.
- [22] M. Delagrammatikas, O. Papadopoulou, P. Vassiliou, Why Does the Addition of Nano-alumina Improve the Performance of Acrylic Coatings Employed in Cultural Heritage Conservation? in: 10th International Symposium on the Conservation of Monuments in the Mediterranean Basin/Natural and Anthropogenic Hazards and Sustainable Preservation. M. Kouli, F. Zezza, D. Kouli (editors). Springer, Cham, 2018, ISBN 978-3-319-78092-4, pp. 115 -125.
DOI: [10.1007/978-3-319-78093-1_11](https://doi.org/10.1007/978-3-319-78093-1_11)
- [23] O. Chiantore, M. Lazzari, Photo-oxidative stability of paraloid acrylic protective polymers, *Polymer*, 42 (2001) pp. 17-27.
DOI: [10.1016/S0032-3861\(00\)00327-X](https://doi.org/10.1016/S0032-3861(00)00327-X)
- [24] J. Monnier, D. Neff, S. Réguer, P. Dillmann, L. Bellot-Gurlet, E. Leroy, E. Foy, L. Legrand, I. Guillot, A corrosion study of the ferrous medieval reinforcement of the Amiens cathedral. Phase characterisation and localisation by various microprobes techniques, *Corros. Sci.* 52 (2010) pp. 695-710.
DOI: [10.1016/j.corsci.2009.10.028](https://doi.org/10.1016/j.corsci.2009.10.028)
- [25] S. Leroy, M. Hendrickson, S. Bauvais, E. Vega, T. Blanchet, A. Dissier, E. Delque-Kolic, The ties that bind: archaeometallurgical typology of architectural crampons as a method for reconstructing the iron economy of Angkor, Cambodia (tenth to thirteenth c.), *Archaeol. Anthropol. Sci.* 10 (2018) pp. 2137-2157.
DOI: [10.1007/s12520-017-0524-3](https://doi.org/10.1007/s12520-017-0524-3)
- [26] Z. Vangelatos, M. Delagrammatikas, O. Papadopoulou, C. Titakis, P. Vassiliou, Finite Element Analysis of the Parthenon marble block- steel clamp system response under acceleration, *ACTA IMEKO*, 10 (2021) pp. 155-165.
DOI: [10.21014/acta_imeko.v10i1.884](https://doi.org/10.21014/acta_imeko.v10i1.884)
- [27] G. J. Varoufakis, The iron clamps and dowels from the Parthenon and Erechthion, *Historical Metallurgy*, 26 (1992), 1-18. Online [Accessed 16 December 2022]
<https://hmsjournal.org/index.php/home/article/view/510>
- [28] E. E. Toumbakari, The Athens Parthenon: Analysis and Interpretation of the structural failures in the orthostate of the northern wall, in: *Structural Analysis of Historic Construction*. D'Áyala & Fodde (editors). Taylor and Francis Group, London, 2008, ISBN 978-0-415-46872-5, pp. 673-681
- [29] G. J. Varoufakis, Metallurgical study of the iron joints of Balanos, Technical Report, YSMA Archive, July 2012. (in Greek).
- [30] E. Labrinou., P. Tsakiridis, G. Papadimitriou, G. Fourlaris, 2015, Laboratory Testing of Metal Joints (Roman Repair) and Metal Joints (Balanos Operation 1923-30). Technical Study M2263, YSMA archive, (in Greek)
- [31] M. Kyritsis-Spinoulas, Behaviour towards corrosion of steel joints and steel joints from the Parthenon restoration 1898-1930, Master thesis, Interdisciplinary Postgraduate Programme Materials Science and Technology, National Technical University of Athens, Athens, 2017 (in Greek).
DOI: [10.26240/heal.ntua.6912](https://doi.org/10.26240/heal.ntua.6912)
- [32] D. de la Fuente, A.J. Alcántara, B. Chico, I. Díaz, J. A. Jiménez, M. Morcillo, Characterisation of rust surfaces formed on mild steel exposed to marine atmospheres using XRD and SEM/ Micro-Raman techniques, *Corros. Sci.* 110 (2016) pp. 253-264.
DOI: [10.1016/j.corsci.2016.04.034](https://doi.org/10.1016/j.corsci.2016.04.034)
- [33] M. Hanesch, Raman spectroscopy of iron oxides and (oxy)hydroxides at low laser power and possible applications in environmental magnetic studies, *Geophys. J. Int.* 177 (2009) pp. 941-948.
DOI: [10.1111/j.1365-246X.2009.04122.x](https://doi.org/10.1111/j.1365-246X.2009.04122.x)
- [34] T. Ohtsuka, S. Tanaka, Monitoring the development of rust layers on weathering steel using in situ Raman spectroscopy under wet-and-dry cyclic conditions, *J. Solid State Electrochem.* 19 (2015) pp. 3559-3566.
DOI: [10.1007/s10008-015-2825-8](https://doi.org/10.1007/s10008-015-2825-8)
- [35] J. Dünwald, A. Otto, An investigation of phase transitions in rust layers using Raman spectroscopy, *Corros. Sci.* 29(9) (1989) pp. 1167-1176.
DOI: [10.1016/0010-938X\(89\)90052-8](https://doi.org/10.1016/0010-938X(89)90052-8)
- [36] S. Li, L.H. Hihara, A Micro-Raman spectroscopic study of marine atmospheric corrosion of carbon steel: The effect of akaganeite, *J. Electrochem. Soc.* 162(9) (2015) pp. C495-502.
DOI: [10.1149/2.0881509jes](https://doi.org/10.1149/2.0881509jes)

- [37] D. L. A. de Faria, S. Venâncio Silva, M. T. de Oliveira, Raman microspectroscopy of some iron oxides and oxyhydroxides, *J. Raman Spectrosc.* 28 (1997) pp. 873-878.
DOI: [10.1002/\(SICI\)1097-4555\(199711\)28:11<873::AID-JRS177>3.0.CO;2-B](https://doi.org/10.1002/(SICI)1097-4555(199711)28:11<873::AID-JRS177>3.0.CO;2-B)
- [38] F. Dubois, C. Mendibide, T. Pagnier, C. Duret, Raman mapping of corrosion products formed onto spring steels during salt spray experiments. A correlation between the scale composition and the corrosion resistance, *Corros. Sci.* 50 (2008) pp. 3401-3409.
DOI: [10.1016/j.corsci.2008.09.027](https://doi.org/10.1016/j.corsci.2008.09.027)
- [39] D. Neff, S. Reguer, L. Bellot-Gurlet, P. Dillmann, R. Bertholon, Structural characterisation of corrosion products on archaeological iron. An integrated approach to establish corrosion forms, *J. Raman Spectrosc.* 35 (2004) pp. 739-745.
DOI: [10.1002/jrs.1130](https://doi.org/10.1002/jrs.1130)
- [40] A Demoulin, C. Trigance, D. Neff, E. Foy, P. Dillmann, V. L'Hostis, The evolution of the corrosion of iron in hydraulic binders analysed from 46- and 260-year old buildings, *Corros. Sci.* 52 (2010) pp. 3168-3179.
DOI: [10.1016/j.corsci.2010.05.019](https://doi.org/10.1016/j.corsci.2010.05.019)
- [41] S. Réguer, P. Dillmann, F. Mirambet, Buried iron archaeological artefacts: Corrosion mechanisms related to the presence of Cl-containing phases, *Corros. Sci.* 49 (2007) pp. 2726-2744.
DOI: [10.1016/j.corsci.2006.11.009](https://doi.org/10.1016/j.corsci.2006.11.009)
- [42] R. A. Nyquist, *Interpreting Infrared, Raman and Nuclear Magnetic Resonance Spectra*, 1st Edition, Academic Press, San Diego, London, 2001, ISBN 0-12-523475-9.
- [43] G. Bailey, The corrosion of a World War one maxim gun mount after 20 years on display. in *Proc. of the AICCM National Conference: Contemporary Collections*, Brisbane, Australia, 17-19 October 2007 pp. 207-211.
- [44] T. Ohtsuka, K. Kubo, N. Sato, Raman spectroscopy of thin corrosion films on iron at 100 to 150 C in air, *Corrosion* 42(8) (1986) pp. 476-481.
DOI: [10.5006/1.3583054](https://doi.org/10.5006/1.3583054)
- [45] X. Du, S. Wang, P. Wang, Q. Gu, J. Xin, Z. Zhang, J. Wang, C. Yao, Characterization of Paraffin-Waxed Apples by Raman Spectroscopy, *Anal. Lett.*, 53(2) (2019) pp.217-227.
DOI: [10.1080/00032719.2019.1643872](https://doi.org/10.1080/00032719.2019.1643872)